

Error Modeling and Simulation for Directional Testing of Space Block

Hongquan Wu¹, Guangling Dong¹, Chi He², Wei Ma¹, Jietao Xie¹, Ruibing Shi¹ and Hongqiang Wei¹

¹Department of Test Technology, Baicheng Ordnance Test Center of China, P. O. Box 108, Baicheng, China

²School of Mechatronic Engineering, CUST, 7089 Weixing Road, Changchun, China

Keywords: Derivative Error Propagation, Monte Carlo, Non-contact Measurement.

Abstract: A directional testing model of space block is studied for effective utilization of optical equipment as theodolite, which gives out the influencing range of testing error on the calculated results. Thus, gifts for guaranteeing actual measuring accuracy and improving testing efficiency are provided. And, the open question in accurate measurement of space block direction can be solved. In this paper, angular information of two different marker points on space block are used for directional testing, through which a partial derivative based error propagation model is built. The rationality and credibility of this model is verified by Monte Carlo simulation. Besides, its calculation results are validated through conventional variance test method in the end. The validation results indicate the rationality and credibility of the partial derivative based error propagation model. The error propagation model can be used to study measuring error distributions on different areas of space block, which lays a firm foundation for optimizing measuring stations distribution, and guarantees measure precision.

1 INTRODUCTION

Research on error modeling and directional testing of space block is primarily focus on measurement calculation of accurate space block axis direction and its error propagation model, which is significant for precision measurement. And takes on wide applied range. For example, initial azimuth angle alignment and maintainance for high accuracy inertial navigation system (INS) require adjusting, assessment and calibration on the system. Besides, as to some long range ground-based weapons with indirect aiming, their shooting accuracy depend directly on loaded initial azimuth data and corresponding calibrated azimuth directional accuracy.

In this paper, the 'space body' refers to the system that has higher directional requirements. Such as the gun barrel axis direction of remote launched weapon system, the axis direction of guided weapon with inertial navigation system, the different parts of ship stitched in accordance with the accurate direction, the different parts of bridge connected in accordance with the accurate direction, etc. The direction testing of these systems is mainly

done by measuring the direction of its axis.

Direction testing for space block axis are generally divided into contact and non-contact types, each with corresponding measuring method. As for non-contact testing type, double theodolites based (Zeng and Lai, 2011) and unit-set total station based (Zeng et al, 2013) measuring methods are frequently-used at present. Some double theodolites based measuring methods bring range information into angle calculation (Shi, 2014).

In most case, space blocks are vehicle-mounted or ship-based, whose azimuth pointing direction can not be given out directly by high precision orientation equipment as turntable. Therefore, measurement and calibration of high precision azimuth pointing direction could only be obtained through non-contact testing with optical equipments as theodolite. In pointing direction testing of space block, factors as electromagnetic environment, installation site, movement process, even atmospheric environment on carrier platform have effects on testing results.

Conventional measuring methods for propagating errors include derivative propagation method and Monte Carlo method. Conventional derivative algorithm takes on different

computational efficiency for different angel measure model. Statistical based Monte Carlo method is suitable for problems difficult to analytical method (Shang and Yang, 2009), whose merits include immune to system complexity and unrestricted by probability distribution types (Liu and Zhao, 2013). Although it can improve computational efficiency under limited calculation counts(Zhang et al, 2010), certain stochastic bias would always exit compared to result of derivative propagation model, which restricts its application on systems requiring high precision measurement.

In actual testing process, there are many errors influencing test results, such as theodolite precision (Fang et al, 2013), tri-axial mechanical error in machining and installation (Li and Wang, 2010), shaft encoder error, human operation error, etc. So, no matter in Monte Carlo simulation or in partial derivative error propagation calculation, rational error source choice is of vital importance.

Common used method in test scheme selection is to choose an optimal specific station site (Zhang et al, 2011). In actual testing process, when optimized station distribution regions for different working conditions of system under test are given out, we just need to select station site on the public area. In this way, frequent setting up of instruments is avoided, which not only guarantees measure precision, but also improves working efficiency.

In conclusion, a directional testing model of space block for effective utilization of optical equipment as theodolite would be studied in this paper, which would give out the error influencing model for making rational testing scheme, reducing error influence and realizing high precision measurement. Thus, pointing direction measurement model of space block and corresponding error propagation model are built, whose simulation model are realized by object-oriented programming language C++. The rationality of error propagation model is demonstrated through simulation, which provides some basis for further research.

2 DOUBLE-THEODOLITES BASED MEASURING METHOD

Directional testing of space block is basically angular variation measurement of a spacial line segment between start and stop position, which can be classified into contact and non-contact types. Contact measurement can be realized through turntable or installed high precision INS, and setting

up theodolite directly on space block can also be used.

In order to solve the disadvantages in contact and non-contact types of measurement, we take full advantage of angle information from non-contact double theodolites intersection measurement to build angle calculation model without distance parameter. In addition, the corresponding error propagation model is studied, whose calculated results are used to prove the feasibility and rationality of the built model.

2.1 Angle Calculation Model

With known connection line of two theodolites and pointing direction of standard base line, directional information of space block can be obtained from its azimuth and elevation angles relative to base line of theodolites. As shown in Figure 1, theodolite 1 should measure azimuth angles α_1, α_2 and elevation angles γ_1, γ_2 on maker points a, b . While theodolite 2 should measure azimuth angles β_1, β_2 on maker points a, b . Thus, the calculation model can be described as follows: model inputs include theodolites measured angles $\alpha_1, \alpha_2, \beta_1, \beta_2, \gamma_1, \gamma_2$ on maker points, while model outputs include azimuth angle ε and elevation angle α of space block to theodolites base line.

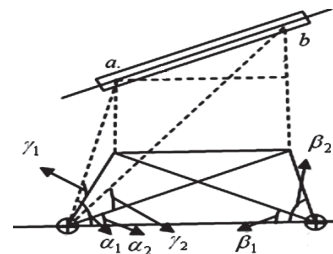


Figure 1: Schematic diagram of azimuth and elevation angle calculation.

Calculation model:

$$\begin{aligned}
 y_1 &= \tan \alpha_2 \tan \beta_2 (\tan \alpha_1 + \tan \beta_1) \\
 y_2 &= \tan \alpha_1 \tan \beta_1 (\tan \alpha_2 + \tan \beta_2) \\
 y_3 &= \tan \alpha_1 \tan \beta_2 - \tan \beta_1 \tan \alpha_2 \\
 \alpha &= \arctan\left(\frac{y_1 - y_2}{y_3}\right) \quad (1) \\
 x_1 &= \sin \beta_2 \tan \gamma_2 \sin(\alpha_1 + \beta_1) \\
 x_2 &= \sin \beta_1 \tan \gamma_1 \sin(\alpha_2 + \beta_2) \\
 x_3 &= \sin^2 \beta_1 \sin^2(\alpha_2 + \beta_2)
 \end{aligned}$$

$$\begin{aligned}
 x_4 &= \sin^2 \beta_2 \sin^2(\alpha_1 + \beta_1) \\
 x_5 &= 2 \sin \beta_1 \sin \beta_2 \cos(\alpha_1 - \alpha_2) \\
 x_6 &= \sin(\alpha_1 + \beta_1) \sin(\alpha_2 + \beta_2) \\
 \varepsilon &= \arctan\left(\frac{x_1 - x_2}{\sqrt{x_3 + x_4 - x_5 \cdot x_6}}\right) \quad (2)
 \end{aligned}$$

Where α denotes Azimuth angle of space block. ε denotes elevation angle of space block.

2.2 Calculation Model Validation

Pointing direction of vehicle-mounted space block is measured and calculated with this method, where some vehicle takes on INS. Comparing the calculated azimuth and elevation angles with those given by direction-finding system (as shown in Table 1 and Table 2), we can see that the calculation results meet the requirement, which indicates the rationality of the built angel measure model.

Table 1: Comparison of azimuth angles from calculation model and direction-finding system.

No.	X1 (mrad)	X2 (mrad)	error (mrad)
1	5782.353	5782	0.353
2	5332.291	5332	0.291
3	232.468	232	0.468
4	232.587	232	0.587

In Table 1, X1 is calculated azimuth pointing direction of space block. X2 is pointing direction of vehicle-mounted direction-finding system.

Table 2: Comparison of elevation angles from calculation model and direction-finding system.

No.	X3 (mrad)	X4 (mrad)	error (mrad)
1	890.707	890	0.707
2	890.674	890	0.674
3	750.024	750	0.024
4	890.022	890	0.022

In Table 2, X3 is calculated elevation pointing direction of space block. X4 is pointing direction of vehicle-mounted direction-finding system.

3 ERROR PROPAGATION CALCULATION MODEL

Thus, we establish the angel measure model and corresponding measuring method for pointing

direction of space block based on non-contact type of method with double-theodolites, which is mainly used in pointing direction testing of space block with complex carrier platform. In actual testing process, system software control precision and hardware factors as carrier motion state, atmospheric environment, electromagnetic environment, servo system precision of carrier platform, sensor accuracy, backlash, base-ring deformation influence measurement precision for pointing direction of space block. Meanwhile, influences of theodolite error and pointing error on measurement precision are not negligible. All the influencing factors are displayed through space block pointing direction error of measurement calculation model. Determining the induced error of different influencing factors on pointing direction of space block is an important problem for precision measurement of pointing direction, which also plays an important role in subsequent research on optimal station distribution. As to optimizing of station distribution scheme, optimum seeking of a specific station site is a common used method. By now, no literature has been found on how to get a feasible station distribution region with satisfied precision according to error distribution range.

On above-mentioned conditions, corresponding angel measure model is built first in this paper. Then, relevant error model is studied on its scientificity and rationality in simulation, which lays a solid foundation for subsequent study on error distribution range. Thus, it provides good pre-study for choosing a big enough station distribution area under required precision.

3.1 Random Error Propagation Calculation of Azimuth Angle

In equation (1), let

$$\tan \alpha = A = \frac{X}{Y}$$

Where X is numerator, Y is denominator.

Taking partial derivatives, the results are shown in the following:

$$\frac{\partial \alpha}{\partial \alpha_1} = \sec^2 \alpha_1 \tan \alpha_2 \tan \beta_1 \frac{(\tan \beta_2 - \tan \beta_1)(\tan \alpha_2 + \tan \beta_2)}{(1 + A^2)Y^2}$$

$$\frac{\partial \alpha}{\partial \alpha_2} = \sec^2 \alpha_2 \tan \alpha_1 \tan \beta_2 \frac{(\tan \beta_1 - \tan \beta_2)(\tan \alpha_1 + \tan \beta_1)}{(1 + A^2)Y^2}$$

$$\frac{\partial \alpha}{\partial \beta_1} = \sec^2 \beta_1 \tan \alpha_1 \tan \beta_2 \frac{(\tan \alpha_1 - \tan \alpha_2)(\tan \alpha_2 + \tan \beta_2)}{(1 + A^2)Y^2}$$

$$\frac{\partial \alpha}{\partial \beta_2} = \sec^2 \beta_2 \tan \alpha_2 \tan \beta_1 \frac{(\tan \alpha_2 - \tan \alpha_1)(\tan \alpha_1 + \tan \beta_1)}{(1 + A^2)Y^2}$$

$$\eta_1 = \left(\frac{\partial \alpha}{\partial \alpha_1} \right)^2 \quad \eta_2 = \left(\frac{\partial \alpha}{\partial \alpha_2} \right)^2$$

$$\eta_3 = \left(\frac{\partial \alpha}{\partial \beta_1} \right)^2 \quad \eta_4 = \left(\frac{\partial \alpha}{\partial \beta_2} \right)^2$$

Substituting above results into error propagation expression, we get equation (3).

$$\sigma_\alpha = \sqrt{\eta_1 \sigma_{\alpha_1}^2 + \eta_2 \sigma_{\alpha_2}^2 + \eta_3 \sigma_{\beta_1}^2 + \eta_4 \sigma_{\beta_2}^2} \quad (3)$$

Where, 0.0116 mrad are taken for σ_{α_1} , σ_{α_2} , σ_{β_1} , σ_{β_2} .

Where σ_α denotes azimuth error calculated by partial derivative model.

3.2 Random Error Propagation Calculation of Elevation Angle

In equation (2), let

$$\tan \varepsilon = A = \frac{X}{\sqrt{Y}}$$

Where X is numerator, Y is denominator.

Taking partial derivatives, the results are shown in the following:

$$\begin{aligned} \frac{\partial \varepsilon}{\partial \alpha_1} &= \frac{1}{2(1+A^2)\sqrt{Y^3}} [2Y \sin \beta_2 \tan \gamma_2 \cos(\alpha_1 + \beta_1) \\ &\quad - 2X \sin \beta_1 \sin \beta_2 \sin(\alpha_2 + \beta_2) \cos(2\alpha_1 + \beta_1 - \alpha_2) \\ &\quad - X \sin^2 \beta_2 \sin 2(\alpha_1 + \beta_1)] \end{aligned}$$

$$\begin{aligned} \frac{\partial \varepsilon}{\partial \alpha_2} &= \frac{1}{2(1+A^2)\sqrt{Y^3}} [-2Y \sin \beta_1 \tan \gamma_1 \cos(\alpha_2 + \beta_2) - \\ &\quad - 2X \sin \beta_1 \sin \beta_2 \sin(\alpha_1 + \beta_1) \cos(2\alpha_2 + \beta_2 - \alpha_1) \\ &\quad - X \sin^2 \beta_1 \sin 2(\alpha_2 + \beta_2)] \end{aligned}$$

$$\begin{aligned} \frac{\partial \varepsilon}{\partial \beta_1} &= \frac{1}{2(1+A^2)\sqrt{Y^3}} [2Y \sin \beta_2 \tan \gamma_2 \cos(\alpha_1 + \beta_1) \\ &\quad - X(\sin 2\beta_1 \sin^2(\alpha_2 + \beta_2) + \sin 2(\alpha_1 + \beta_1) \sin^2 \beta_2 \\ &\quad - 2\sin \beta_2 \sin(\alpha_2 + \beta_2) \cos(\alpha_1 - \alpha_2) \sin(\alpha_1 + 2\beta_1)) \\ &\quad - 2Y \cos \beta_1 \tan \gamma_1 \sin(\alpha_2 + \beta_2)] \end{aligned}$$

$$\begin{aligned} \frac{\partial \varepsilon}{\partial \beta_2} &= \frac{1}{2(1+A^2)\sqrt{Y^3}} [2Y \cos \beta_2 \tan \gamma_2 \sin(\alpha_1 + \beta_1) \\ &\quad - X(\sin^2 \beta_1 \sin 2(\alpha_2 + \beta_2) + \sin^2(\alpha_1 + \beta_1) \sin 2\beta_2 \\ &\quad - 2\sin \beta_1 \sin(\alpha_1 + \beta_1) \cos(\alpha_1 - \alpha_2) \sin(\alpha_2 + 2\beta_2)) \\ &\quad - 2Y \sin \beta_1 \tan \gamma_1 \cos(\alpha_2 + \beta_2)] \end{aligned}$$

$$\frac{\partial \varepsilon}{\partial \gamma_1} = \frac{\sec^2 \gamma_1 \sin \beta_1 \sin(\alpha_2 + \beta_2)}{(1+A^2)\sqrt{Y}}$$

$$\frac{\partial \varepsilon}{\partial \gamma_2} = \frac{\sec^2 \gamma_2 \sin \beta_2 \sin(\alpha_1 + \beta_1)}{(1+A^2)\sqrt{Y}}$$

$$\varepsilon_1 = \left(\frac{\partial \varepsilon}{\partial \alpha_1} \right)^2 \quad \varepsilon_2 = \left(\frac{\partial \varepsilon}{\partial \alpha_2} \right)^2 \quad \varepsilon_3 = \left(\frac{\partial \varepsilon}{\partial \beta_1} \right)^2$$

$$\varepsilon_4 = \left(\frac{\partial \varepsilon}{\partial \beta_2} \right)^2 \quad \varepsilon_5 = \left(\frac{\partial \varepsilon}{\partial \gamma_1} \right)^2 \quad \varepsilon_6 = \left(\frac{\partial \varepsilon}{\partial \gamma_2} \right)^2$$

Substituting above results into error propagation expression, we get equation (4).

$$\sigma_\varepsilon = \sqrt{\varepsilon_1 \sigma_{\alpha_1}^2 + \varepsilon_2 \sigma_{\alpha_2}^2 + \varepsilon_3 \sigma_{\beta_1}^2 + \varepsilon_4 \sigma_{\beta_2}^2 + \varepsilon_5 \sigma_{\gamma_1}^2 + \varepsilon_6 \sigma_{\gamma_2}^2} \quad (4)$$

Where, 0.0116 mrad are taken for σ_{α_1} , σ_{α_2} , σ_{β_1} , σ_{β_2} , σ_{γ_1} , σ_{γ_2} .

Where σ_ε denotes elevation error calculated by partial derivative model;

4 MONTE CARLO SIMULATION

Partial derivative based error propagation model describes the error transmission in calculation model, which causes influence on model outputs by computing process. It takes on concise form, and theoretically should be the expected value after an infinite number of actual testing. So, it is impractical to validate the error propagation model through limited actual measurements. Besides, the

calculation model takes on 6 input variables, whose combination modes are extremely complicated in actual working process. Therefore, model validation is very difficult. In this paper, we use Monte Carlo method to validate the rationality and scientificity of error propagation model. It takes on wide universality and uses direct simulation, which is very suitable for problem difficult to analytical method.

4.1 Working Steps of Monte Carlo Method

The working steps of Monte Carlo are following:

- (1) Simulating sufficient large size of normal distributed observed value of theodolite.
- (2) Substituting the simulated data into pointing direction calculation model of space block to get the corresponding elevation and azimuth angles, calculating the statistical results of azimuth propagation error and elevation propagation error.
- (3) Validating error propagation calculation model.

4.2 Analysis of Model Input Error

Many error sources influence measurement calculation results in this method. For example, common used electronic theodolite in actual testing has many errors influencing test results, such as mechanical errors in machining and installation of vertical axis, pitch axis, and optical axis, shaft encoder error, human operation error, etc. Generally, precision of measurement results is mainly determined by theodolite accuracy.

Therefore, error sources having major influence on model input and general character are selected, such as angel measure error of theodolite, centering alignment error and sighting error.

Table 3: Error sources and their distribution law.

No.	Error source	Distribution law	Standard deviation
1	α_1	Normal distribution	2.5"
2	α_2	Normal distribution	2.5"
3	β_1	Normal distribution	2.5"
4	β_2	Normal distribution	2.5"
5	γ_1	Normal distribution	2.5"
6	γ_2	Normal distribution	2.5"

Generally, angel measure error of theodolite is 2", centering alignment error and sighting error is 1.5", whose composite error is shown in the following expression.

$$\sigma = \sqrt{2^2 + 1.5^2} = 2.5''$$

Model inputs are constructed according to above distribution law and statistic character of error source. Then calculation model (1), (2) are used to carry out Monte Carlo simulations from 1 to 780. So, statistical calculation for propogated error of azimuth and elevation angles can be obtained serially. Under same calculation conditions, propagated error of azimuth and elevation angles can also be calculated from the built error propagation model. Thus, we can make a comparison for two calculation results.

Calculation example 1: vertical distance of theodolites is 3m, with 4m lateral deviation to the right, the calculating results for propogated error of azimuth and elevation angles when Monte Carlo simulation runs up to 780 times.

Table 4: Calculating results of calculation example 1.

Model 1	Model 2				
1	10	50	100	500	780
0.023	0.019	0.02	0.025	0.023	0.024
0.044	0.065	0.039	0.045	0.043	0.044

Calculation example 2: vertical distance of theodolites is 3 m, with 4 m lateral deviation to the left, the calculating results for propogated error of azimuth and elevation angles when Monte Carlo simulation runs up to 780 times. The first line is elevation angle calculation results, the second line is azimuth angle calculation results, and both units are mrad.

Table 5: Calculating results of calculation example 2.

Model 1	Model 2				
1	10	50	100	500	780
0.025	0.024	0.028	0.024	0.024	0.025
0.031	0.022	0.035	0.029	0.032	0.032

In Table 4 and Table 5, Model 1 is partial derivative based error propagation model. Model 2 is Monte Carlo model. The second line is counts of calculation. The third line is elevation angle calculation results, the fourth line is azimuth angle calculation results, and both units are mrad. It can be seen from Table 4 and Table 5 that with the increase

of Monte Carlo simulation times, the calculated propagated error approaches the result of partial derivative based error propagation model. Some results are in accordance with those of partial derivative based error propagation model, while some show certain fluctuation. As in Table 4, propagated error of elevation angles with 780 times simulation is 0.024, yet partial derivative based error propagation model gives 0.023. Namely, there exists minor difference. In the following, we proceed with credibility analysis of above-mentioned two models, and proving the rationality of partial derivative based error propagation calculation model.

5 RESULTS CALCULATION AND ANALYSIS OF TWO MODELS

Since it is inefficient and impractical to validate the rationality of partial derivative based error propagation model with large numbers of actual test, Monte Carlo model for error propagation is built. According to statistical property of Monte Carlo method, high credible results can be obtained with large enough size of simulation tests. That is, its consistency to partial derivative based error propagation model can be checked by certain numbers of Monte Carlo simulations. So, the rationality of partial derivative based error propagation model can be validated. Thus, the problem is summarized into consistency check for calculation results of Monte Carlo model and partial derivative based error propagation model under certain confidence level, where they belong to same population with unknown mean and variance.

5.1 Chi-square Test for Two Error Propagation Models

Suppose X_1, X_2, \dots, X_i represent actual measured values or calculated values in Monte Carlo simulation. X denotes samples following normal distribution $N(\mu, \sigma^2)$, \bar{X} and S_a^2 are sample mean and variance respectively, construct following statistics.

$$\chi^2 = \frac{(n-1)S_a^2}{\sigma_\alpha^2}$$

$$\frac{(n-1)S_a^2}{\sigma_\alpha^2} \sim \chi^2(n-1)$$

Where S_a denotes propagation error calculated by Monte Carlo simulation. σ_α denotes propagated

azimuth error calculated by partial derivative based error propagation model. Then the problem can be describes as follows: for a given confidence level $1-\alpha$, rejection region W: $\chi^2 \leq \chi_{\alpha/2}^2$ or $\chi^2 \geq \chi_{1-\alpha/2}^2$

Hypothesis testing H: whether $\sigma = \sigma_\alpha$
Namely

$$P(\chi^2 \leq \chi_{\alpha/2}^2 \cup \chi^2 \geq \chi_{1-\alpha/2}^2) = \alpha$$

Where σ_α denotes propagated azimuth error calculated by error propagation model. σ denotes overall propagation error calculated by simulation samples (i.e. standard deviation of population).

Hypothesis testing for elevation propagation error can be carried out according to that of azimuth angle. Chi-square tests for propagated error of azimuth and elevation angles in calculation example 1 are realized according to methods introduced above. With a given confidence level $1-\alpha = 0.99$, statistics and its rejection region are calculated from simulation counts 2 to 781. Sequences L1 and L3 in Figure 2 and Figure 3 are curves corresponding to simulation counts, where rejection region lies above L1 and below L3.

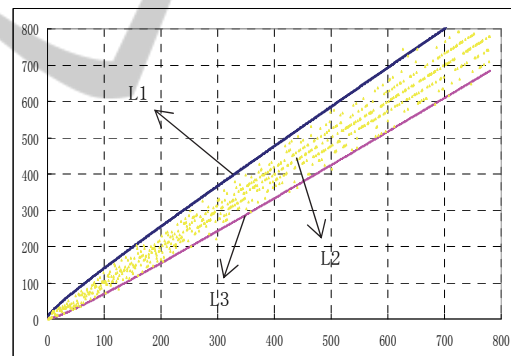


Figure 2: Chi-square test results for propagated error of simulated azimuth angle under confidence level 99%.

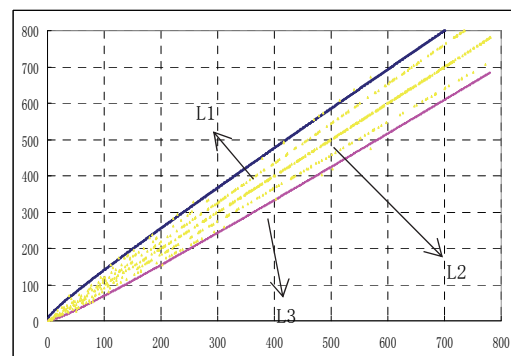


Figure 3: Chi-square test results for propagated error of simulated elevation angle under confidence level 99%.

Chi-square test statistics and rejection region under confidence level 99% are shown in Figure 2 and Figure 3, where horizontal axis represents simulation counts, and vertical axis represents value of Chi-square statistics. Sequence L2 is Chi-square statistics under test, L1 and L3 are boundaries of rejection region, as shown in Figure 2 and Figure 3. L2 lies between L1 and L3, namely outside rejection region, so we can take $\sigma = \sigma_\alpha$. The same results can be obtained for propagated error of simulated elevation angle.

5.2 Propagated Error Variation Range Analysis of Two Models

According to above-mentioned results, $\frac{(n-1)S_\alpha^2}{\sigma^2} \sim \chi^2(n-1)$ can be obtained from $\frac{(n-1)S_\alpha^2}{\sigma_\alpha^2} \sim \chi^2(n-1)$ and $\sigma = \sigma_\alpha$.

As to confidence level $1-\alpha = 0.99$,

$$P(\chi_{\alpha/2}^2/(n-1) \leq \frac{(n-1)S_\alpha^2}{\sigma^2} \leq \chi_{1-\alpha/2}^2/(n-1)) = 1-\alpha = 0.99$$

Namely

$$P\left(\frac{\chi_{\alpha/2}^2(n-1)\sigma^2}{n-1} \leq S_\alpha^2 \leq \frac{\chi_{1-\alpha/2}^2(n-1)\sigma^2}{n-1}\right) = 0.99$$

Thus, we can get the confidence interval of S_α under confidence level $1-\alpha = 0.99$:

$$\left[\sigma \sqrt{\frac{\chi_{\alpha/2}^2(n-1)}{(n-1)}}, \sigma \sqrt{\frac{\chi_{1-\alpha/2}^2(n-1)}{(n-1)}} \right]$$

Table 6: Calculating results of calculation example 3.

Project name	Monte Carlo simulation (counts)				
	10	50	100	500	780
Azimuth lower limit	0.009	0.024	0.029	0.037	0.038
Azimuth upper limit	0.110	0.069	0.061	0.051	0.049
Elevation lower limit	0.003	0.126	0.015	0.019	0.020
Elevation upper limit	0.066	0.037	0.032	0.027	0.026

Calculation example 3, given $1-\alpha = 0.99$, confidence interval to different simulation counts are calculated for calculation example 1 according to above

method, whose results are shown in Figure 4 and Figure 5.

The calculation result unit of Table 6 is mrad. According to confidence intervals of azimuth and elevation angles for calculation example 1 under different simulation counts given in Table 6, we can see that the calculated propagation error by Monte Carlo simulation in Table 4 lie in confidence interval.

In Figure 4 and Figure 5, horizontal coordinates denote simulation counts, vertical coordinates denote propagated error (expressed with mean square error), upper curve (sequence L1) and lower

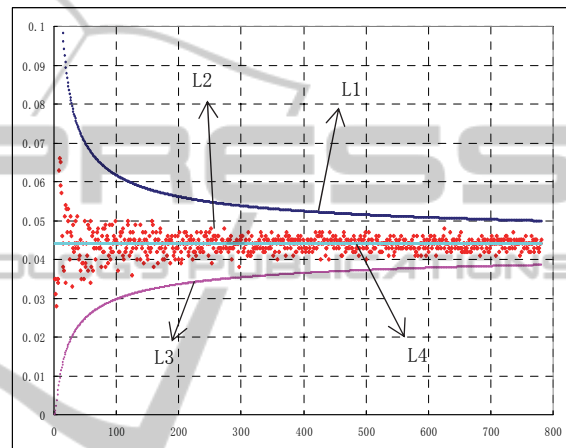


Figure 4: Simulation results comparison for propagated error of azimuth angle under confidence level 99%.

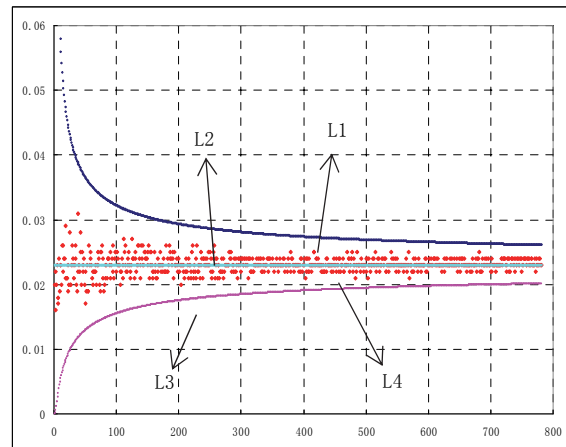


Figure 5: Chi-square test results for propagated error of simulated elevation angle under confidence level 99%.

curve (sequence L3) are boundaries of confidence interval, middle line (sequence L4) is result calculated by partial derivative based error propagation model, scatter diagram (sequence L2) is propagation error corresponding to different

simulation counts.

Propagated error of azimuth and elevation angle from Monte Carlo simulation and partial derivative based model are shown in Figure 4 and Figure 5, where boundary changes for calculation results of Monte Carlo simulation are also given out. The following conclusions can easily be drawn from Figures: the calculated propagation error from Monte Carlo simulation will tend to that of partial derivative based error propagation model as simulation counts increase; the calculated propagation error from Monte Carlo simulation always lie in confidence interval; values in confidence interval tend to those calculated by partial derivative based error propagation model with increment of simulation counts. Obviously, the calculated values from Monte Carlo simulation and partial derivative based model take on consistency. AS uncertainties always exist in Monte Carlo simulation, and high precision system requires both accuracy and consistency for calculation results. So, the more simulation counts, the better calculation results we can obtain from Monte Carlo method. Above Figures show that under confidence level 99%, confidence interval gets short with increase of simulation counts. That is upper and lower boundaries of propagation error from Monte Carlo simulation converge to partial derivative based calculation value, which further demonstrates the rationality and credibility of the built partial derivative based error propagation model.

6 CONCLUSIONS

Although Monte Carlo method takes on good operation, its calculation results have some uncertainty. While precision requirement of system under test is high, we need a propagated error calculation result with good consistency and high precision. So, thousands of simulating calculation is impracticable. The partial derivative based error propagation model built in this paper improves computational efficiency under required error propagation precision, whose rationality is validated by Monte Carlo simulation.

In this paper, we studied a double-theodolites based non-contact pointing direction measuring and calculation method of space block, and built a partial derivative based error propagation model. Also, Monte Carlo statistical test method is used in error propagation modelling, which also validates the rationality of the established partial derivative based error propagation model. The results show that the

partial derivative based model takes on high credibility, which provides basis for further research on calculated pointing direction error distribution of space block. Thus, it can be used in high precision directional testing of space block.

REFERENCES

- Fang, A. G., Xu, R., and Zhang, J. P. (2013). The comparison study on several survey method of rocket launcher's adjustment accuracy. *Chinese Journal of Gun Launch & Control*, (9), 76-78.
- Liu, Q. W., and Zhao, P. L. (2013). An analysis method of system mission reliability based on Monte Carlo method. *Electronic Product Reliability and Environmental Testing*, 31(5), 17-22.
- Li, P., and Wang, Y. (2010). Gun slaving accuracy measurement unit based on digital theodolite detect. *Fire Control and Command Control*, 35(s8), 96-98.
- Shi, F. (2014). A static accuracy measurement of servo system based on double theodolites. *Shanxi Electronic Technology*, (4), 23-25+43.
- Shang, L. Y., and Yang, S. (2009). Research on the guidance precision distribution method based on the variance analysis. *Flight Dynamics*, 27(3), 93-96.
- Zeng, K., and Lai, W. J. (2011). Gun slaving precision detecting system of double-theodolites. *Ordnance Industry Automation*, (7), 73-75.
- Zeng, K., Lai, W. J., and Lei, Y. N. (2013). Gun slaving accuracy measurement system based on total station apparatus. *Journal of Sichuan Ordnance*, 34(4), 18-28.
- Zhang, G., Zhang, Y. T., Ren, G. Q., and Wang, M. Q. (2010). Precision assessment for gun aiming check system based on Monte-Carlo method. *Journal of Academy of Armored Force Engineering*, 24(3), 41-44.
- Zhang, G., Ren, G. Q., Zhang, Y. T., Fu, J. P., Gao, B., and Chen, H. C. (2011). Research on optimizing disposition method of double theodolites in gun rotated precision detection. *Fire Control and Command Control*, 36(9), 176-179.